J Fail. Anal. and Preven. (2023) 23:1203–1215
https://doi.org/10.1007/s11668-023-01678-9

TECHNICAL ARTICLE—PEER-REVIEWED

Based on Stochastic Resonance to Enhance Micro-Fault Signal Features

Kai Wang · Yuan Cheng · Haowen Zheng · Likai Gao · Zhengyu Feng

Submitted: 8 March 2023 / Accepted: 8 May 2023 / Published online: 22 May 2023
© ASM International 2023

Abstract Stochastic resonance (SR) is an effective approach for weak signal detection. Utilizing a single system for cascading has restrictions for conventional SR. To examine the impact of applying various types of SR on the inter-system generation in the same cascade process, the mixed system cascade stochastic resonance (MSCSR) approach is presented in this study. The improved effect is measured in terms of amplitude and signal-to-noise ratio (SNR), on this basis, proposed stochastic weighted particle swarm optimization algorithm to optimize SR system parameters. The results indicate that the collaboration between different systems leads to changes in the potential well of the cascade process. With the proposed approach, MSCSR, the output amplitude is 3.39 times more than that of the bi-stable cascade system, and the SNR is 3.83 dB higher than that of the tri-stable cascade system. The effect of the method described in this study on weak fault characteristics is noticeably stronger than that of the single SR cascade system method. Meanwhile, the method proposed in this paper has important engineering value for micro-fault diagnosis of rolling bearings.

Keywords Micro-fault · Cascaded stochastic resonance · Enhancement features · PSO

K. Wang · Y. Cheng (✉) · H. Zheng · L. Gao · Z. Feng
School of Mechatronic Engineering, Chengdu University of Technology, Chengdu 610059, China
e-mail: cheng_yuan9@163.com

K. Wang
e-mail: wangkai17@cdut.edu.cn

Introduction

Weak fault detection is a popular issue in fault diagnosis research. Data show that many accidents are caused by not eliminating weak faults early enough [1]; therefore, it is important to conduct fault detection for bearings since they are key components in rotating machinery.

Denoising is often performed during signal processing to achieve feature extraction, for instance, wavelet transform (WT), empirical mode decomposition (EMD), and singular value decomposition (SVD) [2–4], and the proposed improved algorithms [5, 6]. These methods are useful for detecting explicit faults, but for weak signals drowned by noise, methods such as signal decomposition can weaken the useful information in the signal and make weak features more difficult to identify. In recent years, researchers have found that noise can be used to enhance weak signals and effectively extract and identify weak features [7]. Stochastic resonance (SR) is a typical nonlinear processing method that uses noise with distinctive characteristics to enhance weak signals. Instead of the traditional suppression of signal noise, this method relies on the interactions between noise, periodic drive forces, and nonlinear systems to enhance weak signal features. The signal-to-noise ratio (SNR) reaches its maximum value when optimal SR parameter matching is achieved. Researchers have extensively investigated using SR to detect weak signals [8]. Initially, the SR phenomenon was generated by introducing the height of the regulatory potential of the system; later, the SR effect was generated by changing the nonlinear system parameters to bring the state of the system to the resonance point, thereby extracting the weak fault characteristics. Different types of SR systems, such as fractional order [9, 10], bi-stable, asymmetric, multi-stable, periodic potential, and underdamped [11–15] systems, have different characteristics when dealing with weak signals.

Because the SR is bounded by both the linear response theory and adiabatic approximation research theories, when the SR method is applied to engineering signals, it must achieve a parametric transformation to satisfy the small parameter condition by scale variation [16, 17]. Research on using SR to detect weak signals has led to several branches: For example, the study of nonlinear systems has resulted in propulsive coupled multi-stable stochastic resonance systems [18], SR tri-stable systems with high-order delayed feedback [19], piecewise tri-stable stochastic resonance (PTSR) systems [20], and composite tri-stable stochastic resonance (CTSR) systems [21]. The introduction of noise studies has led to Lévy noise and Gaussian noise studies [22, 23]. Intelligent algorithms to optimize SR system parameters include the quantum particle swarm algorithm (QPSO), the whale optimization algorithm (IWOA), the beetle antenna search (BAS), weighted particle swarm optimization (PSO), and the ant colony algorithm [24–26].

With time, more researchers found that weak periodic signals could be successfully detected using algorithmic fusion. Wang et al. [27] proposed a method that combined the SR method with computational sequential analysis, which enhances noise utilization and order amplitude. Gong et al. [28] implemented loose connection identification with subharmonic resonance and adaptive stochastic resonance (ASR). Zhang et al. [29] proposed using EWT with improved adaptive bistatic SR as a weak feature enhancement method and was able to achieve robustness in terms of noise. Mba et al. [30] introduced the integration of SR and hidden Markov modeling (HMM) for a vibration signal using multiple performance metrics as the basis for feature extraction.

However, it is challenging to use the composite algorithms that are challenging mentioned above in real-time applications, and the lack of uniform evaluation metrics causes difficulty in achieving an algorithmic arrangement. In recent years, scholars have implemented weak signal detection methods that use different combinations of the same SR systems, including array-based [31] and coupled [32] systems, and Cui et al. [33] proposed post-processing with EMD using cascaded adaptive second-order three-state stochastic resonance (CASTSR) to achieve quality improvement of the EMD decomposition and efficient extraction of weak features. Li et al. [34] proposed coupled bi-stable systems for the adaptive SR method (ACBSR). Gong T et al. [35] proposed cascaded piecewise linear systems, which accurately extracted weak fault features using different combinations of the same system.

Because of the limitations of the methods described above, this paper proposes a mixed system cascade stochastic resonance (MSCSR) method that can effectively improve the performance of the diagnosis algorithm performance when detecting weak signals and the sensitivity to weak fault signals. In this study, a bi-stable system in the first increase accounted for the cascaded saturation ratio and at the same time considers the enhancement characteristics of using a tri-stable system for weak signals that were simultaneously considered. The two systems were combined, and their performances were evaluated using the SNR and the signal amplitude, respectively. The results show that introducing a cascaded SR system improved performance. According to the validated results, the proposed method can effectively detect and accurately identify weak features in bearings and emphasize the frequency of the identified fault features in the frequency domain.

The rest of the paper is organized into four additional sections. Section "Basic SR Model" introduces SR background theories and optimization algorithm. Section "Optimization Algorithm" introduces the MSCSR method, which uses an intelligent algorithm for the parameter search. Section "Experimental Application" presents an evaluation of the MSCSR performance using simulated signals and experimental data. Section "Conclusion" concludes the paper.

Basic SR Model

In an SR described physical phenomenon, when a system has a small periodic force and a broadband random force acting together, the system response switches between different steady states. According to the SR principle, the existence of an optimal noise intensity, nonlinear system parameters, and periodic currents work together to enhance the weak periodic force, i.e., the phenomenon of using weak periodic signals and the presence of random disturbances in the nonlinear system to enhance the periodic output, as shown in Fig. 1.

The SR model can be described using Eq 1 [8]:

$$\begin{cases} \frac{dx(t)}{dt} = -U\prime(x) + S(t) + N(t) \\ <N(t)> = 0, <N(t), N(0)> = 2D\delta(t) \end{cases} \quad \text{(Eq 1)}$$

where *U(x)* represents the potential function of the nonlinear system, *S(t)* represents the weak periodic signal, and *N(t)* denotes the noise signal. In this study, *U(x)* for the cascade investigation, two systems were employed, as shown in Eq (2) [10, 13]:

Fig. 1 Schematic diagram of SR enhancement

$$U_1(x) = -\frac{1}{2}ax^2 + \frac{1}{4}bx^4$$
$$U_2(x) = \frac{1}{2}\alpha x^2 - \frac{1}{4}\beta x^4 + \frac{1}{6}\gamma x^6 \quad \text{(Eq 2)}$$

where $U_1(x)$ represents a bi-stable systems, and $U_2(x)$ represents tri-stable systems. The parameters a and b in $U_1(x)$ denote the bi-stable system parameters, and the parameters α, β, and γ in $U_2(x)$ denote the tri-stable system's parameters.

Different SR systems share the same implementation mechanism, and this study employs a tri-stable system to demonstrate the idea (using tri-stable systems as a base model to study SR phenomenon). The potential function solution's location is altered by changing the parameters, and this ignites the SR phenomenon by altering the depth of the potential well and the solution's relative position to the solution, which alters how easily the particle jumps between potential wells. The Rangzwan equation is solved, as shown in Eq 3.

$$x_1 = x_5 = \pm\sqrt{\frac{\beta + \sqrt{\beta^2 - 4\alpha\gamma}}{2c}}$$
$$x_2 = x_4 = \pm\sqrt{\frac{\beta - \sqrt{\beta^2 - 4\alpha\gamma}}{2\gamma}}, x_3 = 0 \quad \text{(Eq 3)}$$

where x_2 and x_4 are the tri-stable two unstable steady solutions, while x_1, x_3, and x_5 are the tri-stable steady solutions, the structural parameter of the potential function of the system is α, β, and γ.

The output of the tri-stable system is a Brownian particle jumping motion formed between two different potential wells (a nonlinear system potential function). The width of the potential wells can be described by two tri-stable system solutions. The system particles are constrained within the two potential wells and influenced by the corresponding initial values, while the height of the potential function is influenced by the system parameters, indicating that an optimal SR phenomenon can be achieved by adjusting the system parameters, as shown in Fig. 2.

The output of the potential function is also influenced by the analytical parameters β and γ. In the case of Brownian particles, the potential well can leap more easily as the parameters are increased because the midpoint of the potential well change range is small. On the other hand, it can be determined that changing the parameters α, β, and γ can modify the distance between the potential barrier and the potential well. As the parameter β grows, the jump probability drops.

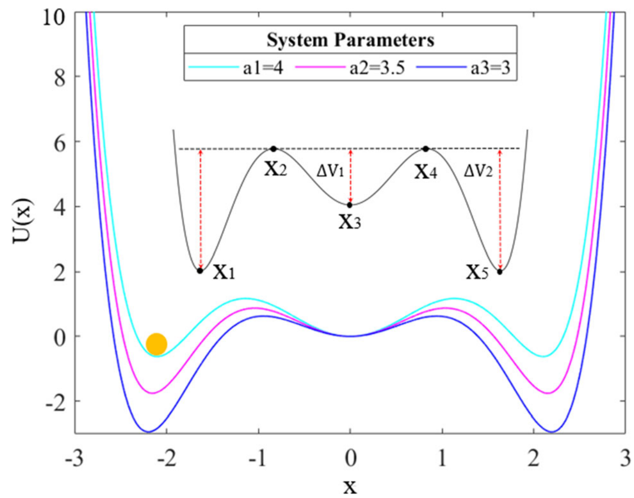

Fig. 2 Relationship between *U(x)* and system parameter a (solution of the potential function and potential wells)

Optimization Algorithm

Finding the ideal system settings is essential for enhancing the SR method's efficiency. However, the correlation between the parameters is poor, it is difficult to obtain the optimal solution to achieve the best SNR output. The relevant parameters are coupled to each joined together, which makes the parameter adjustment difficult; therefore, an intelligent algorithm for parameter seeking was used during this study to improve the efficiency of weak signal detection. In this study, a stochastic weighted PSO algorithm, this algorithm was derived from the stochastic optimization technique for populations, and its algorithmic model can be considered as the foraging behavior of a bird population, by converting the search space into the flight space of the birds. The optimal solution can be found through the collaboration and information sharing by the individuals in the population, according to the following steps:

(1) System parameters, including the learning factor, the number of iterations, the average value of the accompanying weights, and the spatial dimension, initialized. The parameters are also initialized.
(2) The number of iterations required to update the position, and velocity of the particle is input.
(3) The particle fitness function values are evaluated. The output SNR ratio is selected as the fitness function of the evaluation index.
(4) If the condition is satisfied, the iterations are complete, and the global optimum is output; if not, the particle state continues to be updated. The optimal solution can be obtained by this algorithm, as expressed by Eqs 4 and 5 [16]:

$$v_{a,b}(t+1) = wv_{a,b}(t) + c_1r_1(L_{a,b} - x_{a,b}(t)) + c_2r_2(L_{c,b} - x_{a,b}(t)) \quad \text{(Eq 4)}$$

$$x_{a,b}(t+1) = x_{a,b}(t) + v_{a,b}(t+1), b = 1, 2, \cdots, d \quad \text{(Eq 5)}$$

where the inertia weight coefficients are denoted by w, the positive learning coefficients are denoted by c_1 and c_2, r_1 and r_2 represent uniformly distributed random numbers in the interval [0 1], and $L_i = [L_{i,1}, L_{i,2},\ldots, L_{i,d}]$ is the best position found in the neighborhood. Additionally, the velocity interval $[V_{min}, V_{max}]$ and the position interval $[X_{min}, X_{max}]$ can also be used to restrict motion.

$$\begin{cases} w = \mu + \sigma N(0,1) \\ \mu = \mu_{\min} + (\mu_{\max} - \mu_{\min}) rand(0,1) \end{cases} \quad \text{(Eq 6)}$$

The resulting weighted particle swarm algorithm can boost the w-value, accelerate the algorithm, and converge to the desired outcome more quickly. Equation 6 demonstrates approach regulates the w-value and is better suited for use in stochastic resonance parameter search by using the random number 0–1 range for weight summation.

Proposed SR—MSCSR Method

MSCSR Principle

To study the impact of the system's cascade mechanism on the output, a mixed SR cascade methodology is presented in this part. The switching of the system during the cascade process significantly alters the potential function involved in the solution, modifying the output parameters, subject to the optimal system parameters. The bi-stable and tri-stable subsystems were utilized as the subject matter, and simulation results show that adding the bi-stable system to the tri-stable system has an effect similar to that of the tri-stable cascaded system in terms of growth, the method is known as MSCSR, as shown in Fig. 3.

The MSCSR expression for the n-level cascade is shown in Eq 7:

$$\begin{cases} \dfrac{dx_1}{dt} = -\alpha x_1 + \beta x_1^3 - \gamma x_1^5 + ax_1 + bx_1^3 + S(t) + N(t) \\ \dfrac{dx_2}{dt} = -\alpha x_2 + \beta x_2^3 - \gamma x_2^5 + x_1(t) + ax_2 + bx_2^3 \\ \cdots\cdots \\ \dfrac{dx_n}{dt} = -\alpha_n x_n + \beta_n x_n^3 - \gamma_n x_n^5 + x_{n-1}(t) + ax_n + bx_n^3 \end{cases} \quad \text{(Eq 7)}$$

where a and b represent the parameters of the bi-stable SR system, α, β, and γ represent the system parameters of the tri-stable SR system, the simulated sinusoidal signal is represented by S(t), the noise signal is represented by N(t), and this system was a tri-stable cascaded SR system when $a = b = 0$; on the other hand, this system was a bi-stable cascaded SR system when $\alpha = \beta = \gamma = 0$ happens at all levels. When the cascaded form changes, only a single $\alpha = \beta = \gamma = 0$ occurs, at which point the system develops into MSCSR. There are two potential wells for tri-stable system and one for bi-stable system, which can both reflect the process of particle migration in the nonlinear system, by figuring out the two system combined potential well depths, and adjusting the system parameters can produce the best SR, as shown in Eq 8 [36]:

$$\Delta V = -\frac{a^2}{4b}$$
$$\Delta V_1 = \frac{1}{24\gamma_i^2}[(\beta_i^2 - 4\alpha_i\gamma_i)^{\frac{3}{2}} + \beta_i(\beta_i^2 - 4\alpha_i\gamma_i)] \quad \text{(Eq 8)}$$
$$\Delta V_2 = \frac{1}{12\gamma_i^2}(\beta_i^2 - 4\alpha_i\gamma_i)^{\frac{3}{2}}$$

ΔV for the bi-stable potential well, ΔV_1 and ΔV_2 for the tri-stable potential well. The mixed system enables the cascaded SR to adjust both the system parameters and the potential function. The potential well is altered by changing the system parameters, which impacts the particle jumps. It was discovered that the mixed system entry alters the system properties, changing the potential well depth for the cascade process. The output SNR depends on the potential well because different cascade forms will produce various signals, which will vary the output SNR of each step. The output SNR can be described as the ratio of the output signal power P_s to the average power of the

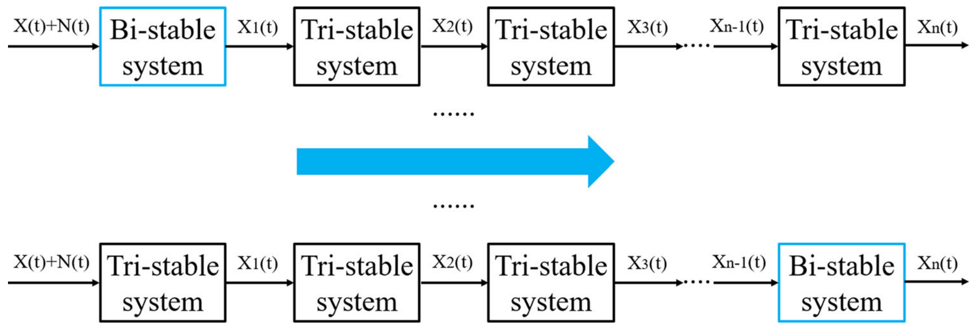

Fig. 3 MSCSR schematic diagram

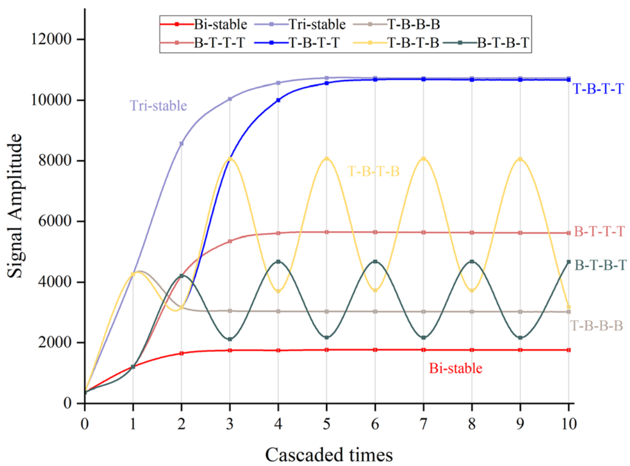

Fig. 4 B represents the bi-stable system, and T represents the tri-stable system. T-B-B-B represents a system in which the tri-stable system is used first, then the bi-stable system is used for cascading, the rest of the matching methods are as described previously

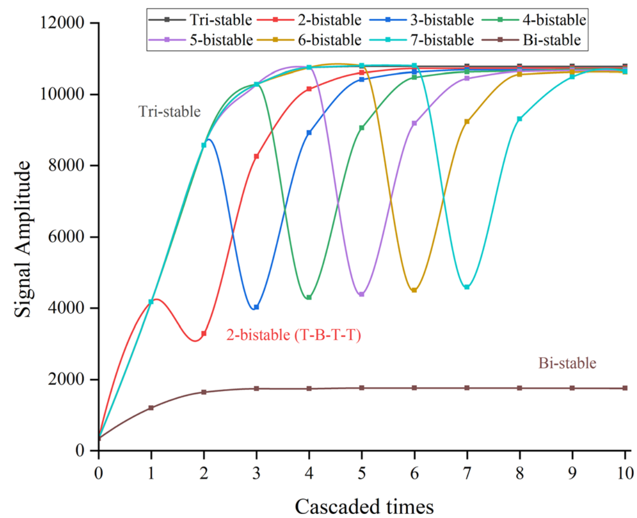

Fig.5 Effect of introducing bi-stable system at different positions on the amplitude output. (i-bi-stable represents the introduction of the ith cascade into the bi-stable system)

background noise spectrum at $G_N\ (w_0)$. The output SNR is shown in Eq 9 [37]:

$$SNR = \frac{\pi}{2}\left(\frac{Ax_m}{D}\right)^2 r_k \Bigg/ \left[1 - \frac{1}{2}\left(\frac{Ax_m}{D}\right)^2 \frac{4r_k^2}{4r_k^2 + w_0^2}\right] \qquad \text{(Eq 9)}$$

where w_0 is the driving frequency, r_k is the particle jump probability (Kramers rate), and x_m is the particle steady-state position. By neglecting the higher-order terms in the denominator of Eq 9, and under the constraints of adiabatic approximation and linear response theory, in which only small parameter signals are applicable, the SNR can be approximated by Eq 10:

$$SNR = \sqrt{2\Delta V}\left(\frac{A}{D}\right)^2 e^{-\frac{\Delta V}{D}} \qquad \text{(Eq 10)}$$

The SNR value is mostly influenced by the potential well value and the noise, as shown in Eq 10; however, random noise in the operating environment is difficult to control, the analysis found that the output SNR can be controlled by improving the potential well value. In contrast with the traditional single cascade form, the method proposed in this section can form a single processing to generate different potential well values, and the output SNR of the nonlinear system is also better than the traditional cascade method. In the following, utilizing simulated signals, the impact of the mixed system on the signal output amplitude and SNR will be investigated.

Model Analysis

Simulation proves that the bi-stable cascaded system increases the amplitude to 95% of the cascaded saturation after the first two SRs. To describe the effects of different cascaded tri-stable and bi-stable system scenarios on the output signal amplitude, the bi-stable system was cascaded with the tri-stable system, using a sinusoidal signal with a frequency of 0.01 Hz and a noise intensity of 0.5, as shown in Fig. 4, to illustrate the effect of various cascaded cases of tri-stable and bi-stable on the output signal amplitude. It was observed that cascaded saturation occurs when the

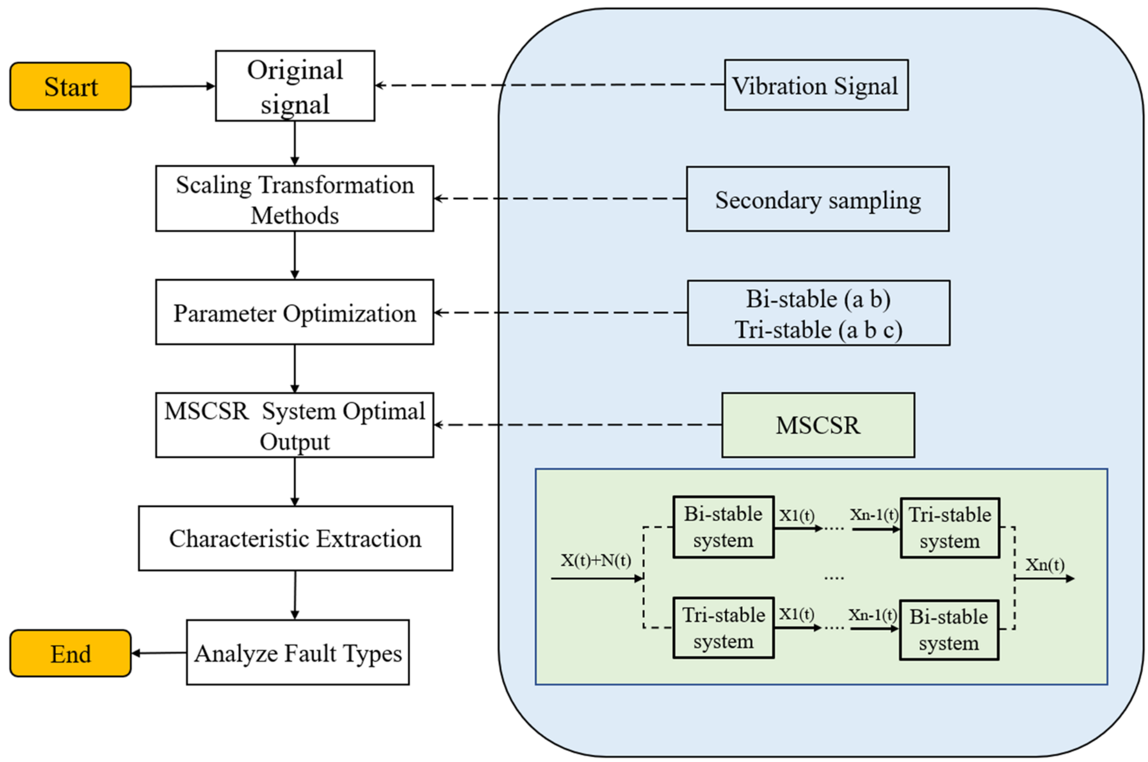

Fig. 6 MSCSR fault identification process flowchart

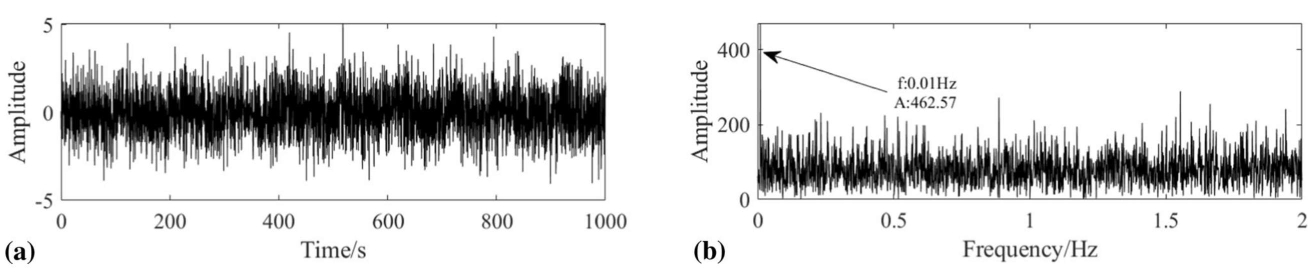

Fig. 7 Simulation signal: (**a**) signal waveform and (**b**) frequency-domain diagram

number of cascades reaches a certain value, at which point the signal output amplitude no longer changes significantly as the number of cascades increases. The effect of various mixed cascades on the output response was observed. However, the use of a B-T-T-T mixed cascaded system produces no significant signal amplitude enhancement, it is easier to highlight weak signals by preferentially using a tri-stable system in the cascaded system. When using the MSCSR method for a second introduction to the bi-stable system, it was found that this method approximates the output amplitude of the best tri-stable system, indicating that this method has a clear advantage for increasing the amplitude. When the MSCSR approach was described for the bi-stable system's second introduction, it was discovered that the method comes close to reproducing the output amplitude of the ideal tri-stable system. The proposed MSCSR method introduction of the bi-stable system will cause a temporary drop in signal amplitude, but the reintroduction of the tri-stable system will rekindle the sensitivity to weak signals, and the introduction of the bi-stable system to reduce the signal amplitude in the lower level of the tri-stable system will get a significant increase, which is obvious from the second cascaded amplitude gain, as shown in Fig. 4.

The effects of the various cascaded methods on the final signal output amplitude were analyzed, and the analysis results show that the proposed MSCSR method and the tri-stable SR system have the highest, final output amplitude

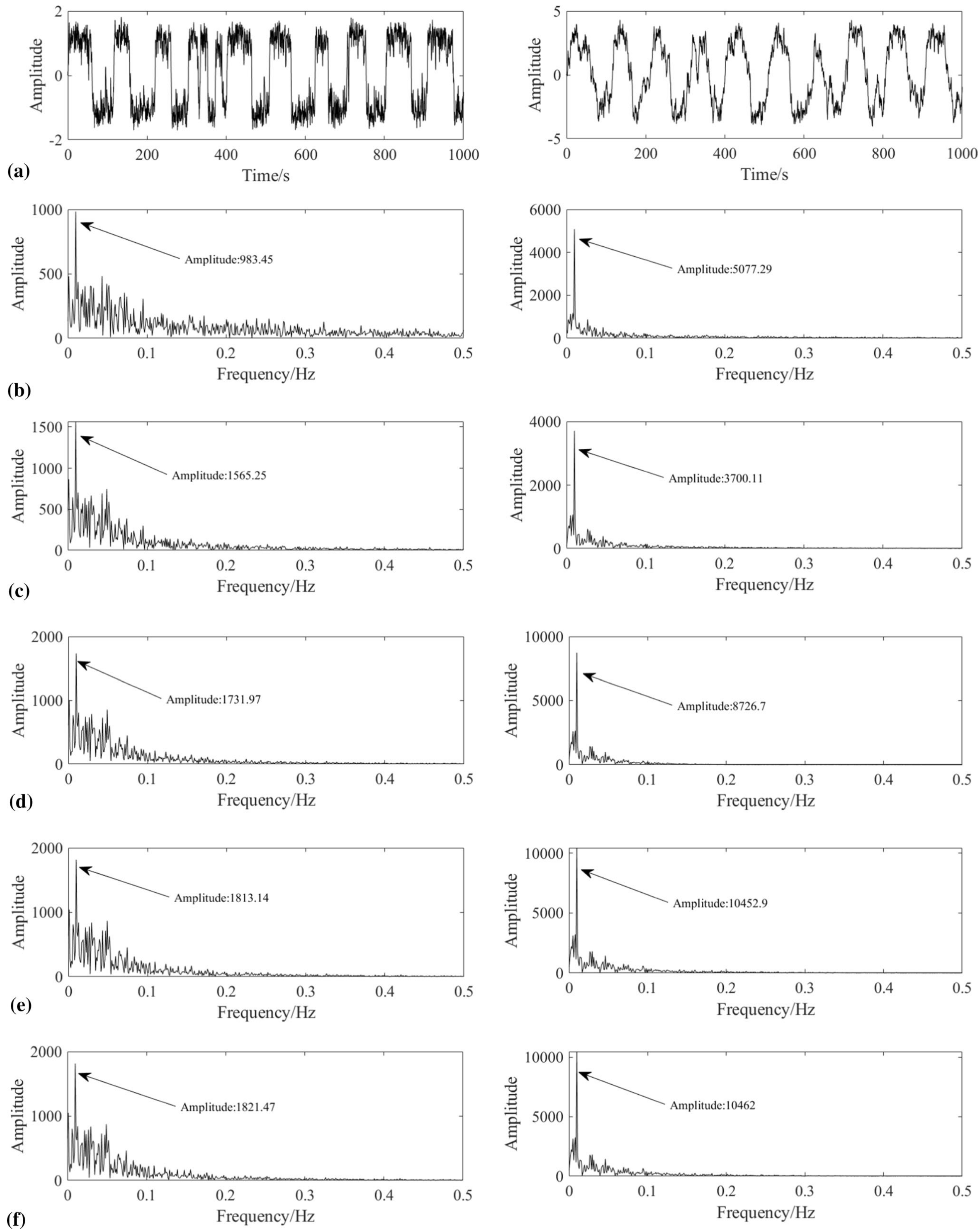
(a)
Amplitude
Time/s
(b)
Amplitude
Frequency/Hz
Amplitude:983.45
Amplitude:5077.29
(c)
Amplitude:1565.25
Amplitude:3700.11
(d)
Amplitude:1731.97
Amplitude:8726.7
(e)
Amplitude:1813.14
Amplitude:10452.9
(f)
Amplitude:1821.47
Amplitude:10462

◀**Fig. 8** Comparison of the bi-stable cascaded system with the amplitude enhancement of the proposed MSCSR method. (**a**) primary cascaded time-domain signal waveform, (**b**) primary cascaded frequency-domain spectrum, (**c**) secondary cascaded frequency-domain spectrum, (**d**) tertiary cascaded frequency-domain spectrum, (**e**) quaternary cascaded frequency-domain spectrum, (**f**) quinary cascaded frequency-domain spectrum. i represents different methods, 1 represents the bi-stable system, and 2 represents the MSCSR method

and that the output amplitude of the interleaved cascaded system also exhibits periodic changes.

The MSCSR system can recover the signal's amplitude no matter where the bi-stable system is inserted. The result of switching between systems might still increase the signal amplitude even when new systems are introduced that reduce it. It is demonstrable that the MSCSR's amplitude augmentation effect is much superior than that of the bi-stable system. The amplitude of MSCSR method will eventually stabilize in a specific range as the number of cascades rose, as shown in Fig. 5. The stochastic weight PSO method is combined with the MSCSR method in this study to search for the ideal system parameters for feature extraction and feature amplification of weak signals, and the real data defect diagnostic process is depicted as shown in Fig. 6.

Simulation Verification and Experimental Application

Simulation Verification

To test the effectiveness of the proposed method and to ensure the usability of the SR method, a small parametric signal was established. This simulated signal was sinusoidal with added white noise. The simulated signal could be described by the equation $X(t) = A\sin\ (2\pi ft) + N(t)$, where f represents the weak signal frequency of 0.01 Hz, and $N(t)$ is the white noise, which satisfies the normal distribution. The fourth-order Runge–Kutta method used to solve for the SR. The results of the PSO search were used to determine the potential function parameters. Calculating the optimal optimum parameters resulted in bi-stable system: parameters of $a = 1.231$ and $b = 0.822$, tri-stable system parameters of $\alpha = 0.0275$, $\beta = 0.0365$, and $\gamma = 0.0017$, and a computational step of $h = 0.25$. The simulation results demonstrate that a weak periodic signal with a frequency of 0.01 Hz can be detected from the noisy signal, as shown in Fig. 7a. There is no information accessible for the time-domain portion, and the periodic signal component is totally masked by the noise. The periodic signal with the original signal fault frequency of 0.01 Hz is identified in the frequency-domain plot, as shown in Fig. 7b, and the signal amplitude at frequency 0.01 Hz is 462.57. However, there are still cluttered frequencies in the high-frequency region, making it difficult to apply the proposed method to engineering signals. Further research is required.

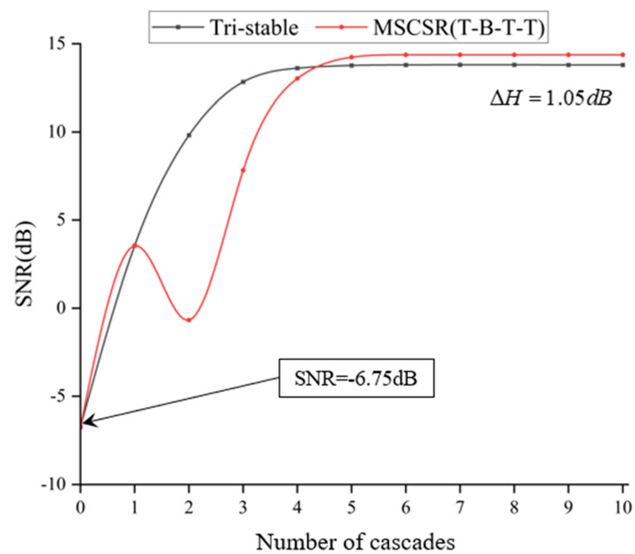

Fig. 9 Tri-stable systems and the MSCSR: the relationship between the number of cascades and SNR

The simulation results show that when the cascaded system reaches a certain number of cascades, the amplitude increase reaches its upper limit, and the enhanced saturation phenomenon occurs. Before SR processing, the amplitude of the frequency-domain spectrum was 462.57, as shown in Fig. 7b. The saturation value of bi-stable system is 1821.47, as shown in Fig. 8f1, and the saturation value of MSCSR is 10462; as shown in Fig. 8f2, the increase in MSCSR is 5.74 times that of bi-stable system, the MSCSR method has a clearer time-domain signal than the bi-stable system, as shown in Fig. 8a1 and a2, and the simulation signal shows that the MSCSR amplitude enhancement was significantly better than that of bi-stable system. Additionally, at a fault frequency of 0.01 Hz, the bi-stable system had difficulty in forming a clear determination area, while the MSCSR method highlighted the fault frequency more for low frequencies and had more prominent advantages when applied to engineering signals.

The SNR was used to measure the enhancement capability of the proposed method for weak signals, and since the SNR changes due to the introduction of random noise, the output error is reduced by averaging the SNR multiple times as shown in Fig. 9. The initial SNR of the simulated signal −6.75 dB, the weak signal with a frequency of 0.01 Hz was completely disturbed by the noise. This figure exhibits the change in the under multiple cascades,

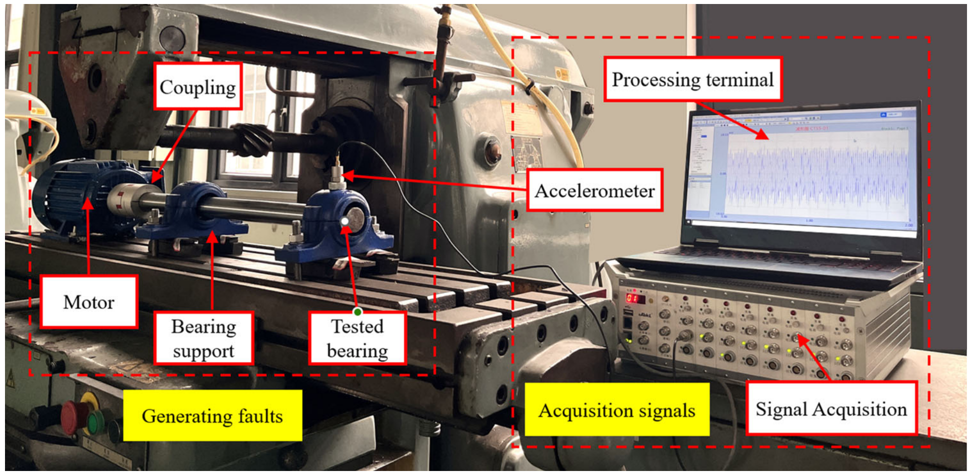

Fig. 10 Fault detection test platform

reducing the noise interference in the experiment, and the data from multiple experiments were then averaged. The introduction of the bi-stable system decreased the SNR, but the tri-stable system enhanced the SNR ratio again, the results show that introducing the bi-stable system MSCSR method produced significant modulation in the output SNR, and the SNR gain changed significantly in the lower level of the tri-stable system and was saturated with the number of cascades. In summary, the MSCSR method has a better weak signal recognition capability.

Experimental Application

To verify the practicality of the proposed method, a comprehensive experimental platform was established for mechanical faults, consisting of fault signal generation and signal acquisition devices, as shown in Fig. 10.

(1) The motor drives the bearing under test through the coupling, with a motor speed of 1240 r/min.
(2) The vibration signal is detected by an accelerometer.
(3) The signal is sampled by an acquisition system (uTeKL-uT89) with a sampling frequency of 12 kHz.
(4) A 1-mm broad, 0.4-mm long, and 0.2-mm deep fault is set in the outer raceway of the bearing, the bearing type was 6207-2RSR, as shown in Fig. 11.

Figure 12a shows that the raw bearing fault data had no obvious periodicity in the time-domain portion. However, in the frequency-domain portion depicted in Fig. 12b, the fault characteristic frequency was overwhelmed by the interference frequency, and the fault frequency could not be accurately identified. The desired characteristic frequency has been completely lost in the real signal frequency-domain range as compared to the interference-free simulated signal. The benefits of the suggested approach are then confirmed in real signals.

According to the bearing outer ring fault characteristic frequency calculation equation, substituted into the bearing specific parameters, as shown in Table 1, the calculation can be obtained from the characteristic frequency of 74.772. The original signal from the bi-stable cascaded SR system initially had periodic characteristics in the time domain, as shown in Fig. 12c, the fault frequency of 74.772 Hz is accurately identified in the frequency-domain portion, but there was still rich frequency information in the low-frequency region, as shown in Fig. 12d, which caused difficulty in identifying the fault accurately; meanwhile, the spectrum diagram also shows the failure signal multiplier.

Similarly when performing the MSCSR method proposed in this paper, as shown in Fig. 12e, the time-domain portion exhibited obvious periodicity with the pure signal. Additionally, there was less band interference, in the low-frequency band, allowing for clearer identification of the fault characteristic frequency, as shown in Fig. 12f. The bearing fault frequency was 74.772 Hz, and the error with the experimental value of 74.0768 Hz was 0.01%, the bearing failure type can be determined by failure frequency. It is apparent that the proposed method has an advantage in high-frequency processing over the improved method described previously.

It is also verified that the proposed MSCSR method has a better amplitude enhancement than the bi-stable system, with an increase in the intensity of 3.39 times. Calculating the SNR also proved that this method had obvious characteristics that were better than those of the tri-stable system, under the same initial signal conditions, the increase in the SNR of the tri-stable system rose with the number of cascades and eventually stabilized.

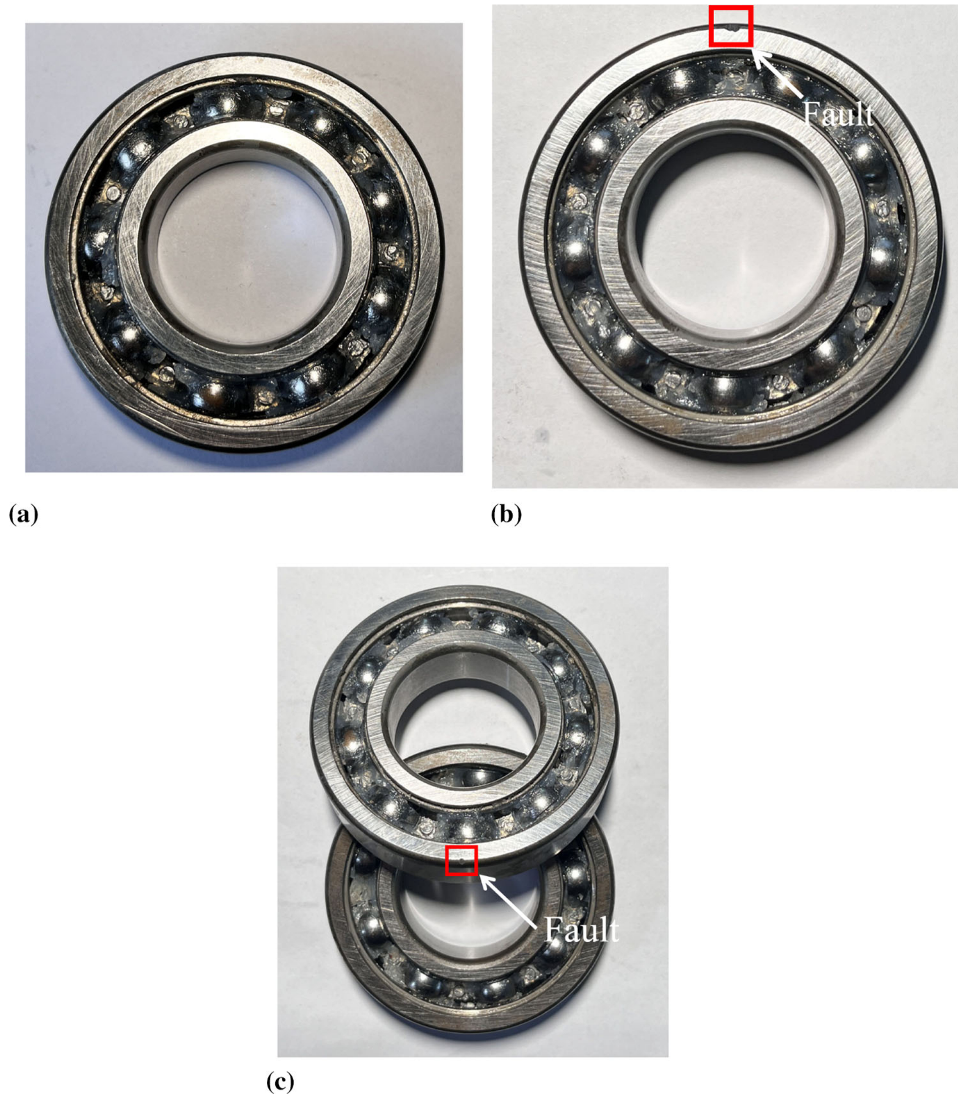

Fig. 11 (**a**) Normal bearing, (**b**) faulty bearing position 1, and (**c**) faulty bearing position 2

The initial fault signal SNR, −40.33 dB, was drowned in the noise. The SNR of the proposed MSCSR method increased with the number of cascades and was improved by 3.83 dB relative to that of the tri-stable system, as shown in Fig. 13. This demonstrates that the proposed method enhances the SNR and can be used for weak signal enhancement.

Comparison Verification

This section discusses a comparison between amplitude increases. For both signals, the real signal is rich in information in each region, and there were interfering signals from the equipment in addition to the added noise. Therefore, it was more likely that there would be an insignificant increase during the actual processing. The simulated signal composition was relatively simpler, and the amplitude increased to 574% of the original using bi-stable cascaded system. For verification of the real signal, the proposed method can still achieve an increase of 339%. This section discusses an SNR enhancement comparison. The SNR is enhanced between the tri-stable cascaded system and the MSCSR system, due to the introduction of the bi-stable system characteristics, for simulated signal and the real acquisition signal, the proposed method outperformed the tri-stable cascaded system. The enhancement of the SNR by the proposed method was confirmed by the verification of both signals. In conclusion, the amplitude of the proposed MSCSR method increased more than that of the bi-stable cascaded system, and the SNR enhancement was better than that of the tri-stable cascaded system. It was also verified for different

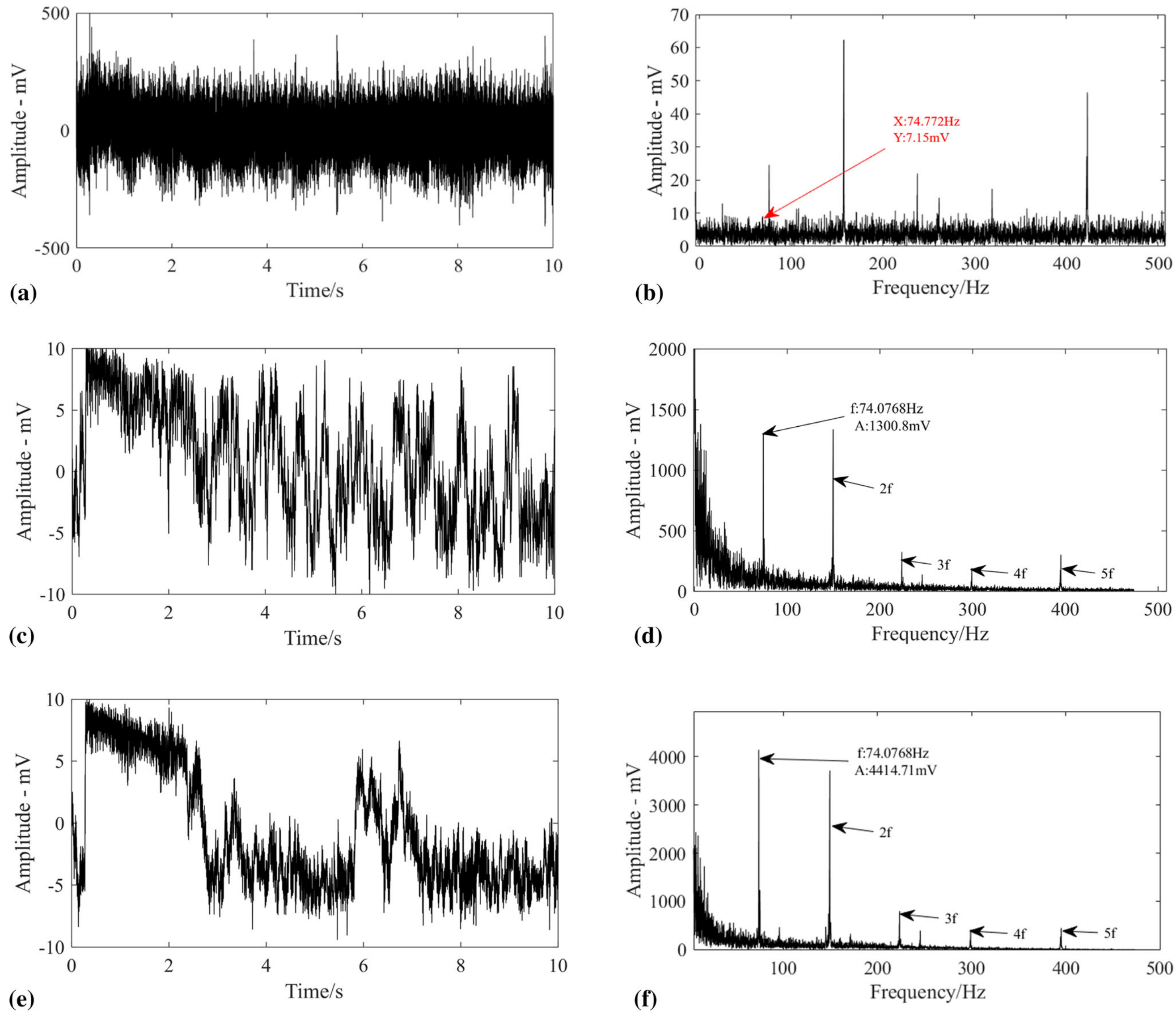

Fig. 12 Raw fault vibration signal: (**a**) signal waveform and (**b**) frequency-domain spectrum. Stochastic Resonance fault diagnosis results for the bi-stable system with MSCSR: (**c**) bi-stable cascaded system time-domain waveform, (**d**) bi-stable cascaded system frequency-domain spectrum, (**e**) MSCSR system time-domain waveform, and (**f**) MSCSR system frequency-domain spectrum

Table 1 Failed bearing parameters

Bearing type	Pitch diameter (mm)	Number of balls (pcs)	Ball diameter (mm)	Contact angle (°)
6207-2RSR	53.5	9	10.5	0

signals, thereby confirming the advantages of the proposed method in extracting weak signal features.

Conclusions

In this study, an MSCSR method was used to extract weak signals from engineering equipment and identify bearing defects. This study produced three primary conclusions.

(1) The cascade saturation phenomenon was introduced into an SR cascaded system, which, in addition to the common amplitude increase saturation, was also present in the SNR rating index.
(2) The proposed MSCSR method provided new treatments by employing different types of SR systems, combining the advantages of various systems in nonlinear treatments. The results showed that the

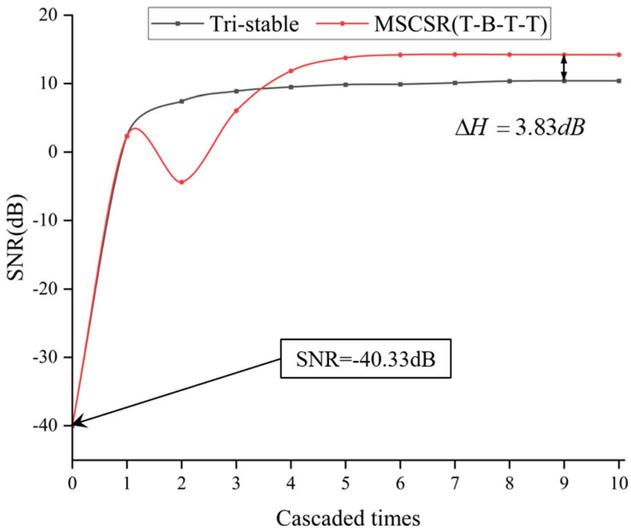

Fig. 13 Tri-stable systems and MSCSR: the relationship between the number of cascades and the SNR

results were better than those of a cascade of the same type of SR systems and provided inspiration for the study of different system cascades.

(3) The sensitivity of the nonlinear system to the parameters was exploited to achieve an increase in the amplitude and the SNR. The results of analyses of two types of signals showed that the proposed method could accurately detect weak signals disturbed by noise as well as enhance the characteristics of weak signals; therefore, this method had the potential for application in the detection of micro-faults.

Acknowledgments The authors thank Professor Engineer Jian Wang from 7th Academy (China Aerospace Corporation) for his guidance on this work. This work was supported by the Sichuan Youth Fund Project (No: SC20220230), the authors also would like to thank the anonymous reviewers for their valuable comments and suggestions. They help us to improve the work comparatively and fundamentally.

Conflict of interest The authors declare no conflict of interest in preparing this article.

References

1. Z. Gao, X. Liu, An overview on fault diagnosis, prognosis and resilient control for wind turbine systems. Processes. **9**(2), 300 (2021). https://doi.org/10.3390/pr9020300
2. G. Yan, J. Chen, Y. Bai et al., A survey on fault diagnosis approaches for rolling bearings of railway vehicles. Processes. **10**(4), 724 (2022). https://doi.org/10.3390/pr10040724
3. S. Wang, P. Niu, Y. Guo et al., Early diagnosis of bearing faults using decomposition and reconstruction stochastic resonance system. Measurement. **158**, 107709 (2020). https://doi.org/10.1016/j.measurement2020.107709
4. L. Xu, S. Chatterton, P. Pennacchi, Rolling element bearing diagnosis based on singular value decomposition and composite squared envelope spectrum. Mech. Syst. Signal Process. **148**, 107174 (2021). https://doi.org/10.1016/j.ymssp.2020.107174
5. Z. Wang, N. Yang, N. Li et al., A new fault diagnosis method based on adaptive spectrum mode extraction. Struct. Health Monit. **20**(6), 3354–3370 (2021). https://doi.org/10.1177/147592172098694
6. Y. Cheng, M. Lin, J. Wu et al., Intelligent fault diagnosis of rotating machinery based on continuous wavelet transform-local binary convolutional neural network. Know. Based Syst. **216**, 106796 (2021). https://doi.org/10.1016/j.knosys.2021.106796
7. Z. Qiao, Y. Lei, N. Li, Applications of stochastic resonance to machinery fault detection: a review and tutorial. Mech. Syst. Signal Process. **122**, 502–536 (2019). https://doi.org/10.1016/j.ymssp.2018.12.032
8. S. Lu, Q. He, J. Wang, A review of stochastic resonance in rotating machine fault detection. Mech. Syst. Signal Process. **116**, 230–260 (2019). https://doi.org/10.1016/j.ymssp.2018.06.032
9. Q.B. Wang, H. Wu, Y.J. Yang, The effect of fractiona-l damping and time-delayed feedback on the stoc-hastic resonance of asymmetric SD oscillator. Nonlinear Dyn. **107**, 1–16 (2022). https://doi.org/10.1007/s11071-021-07105-8
10. X. Zeng, X. Lu, Z. Liu et al., An adaptive fractional stochastic resonance method based on weighted correctional signal-to-noise ratio and its application in fault feature enhancement of wind turbine. ISA Trans. **120**, 18–32 (2022). https://doi.org/10.1016/j.isatra.2021.03.012
11. W. Cheng, X. Xu, Y. Ding et al., An adaptive smooth unsaturated bistable stochastic resonance system and its application in rolling bearing fault diagnosis. Chin. J. Phys. **65**, 629–641 (2020). https://doi.org/10.1016/j.cjph.2020.03.015
12. Z. Li, B. Shi, X. Ren et al., Research and application of wea-k fault diagnosis method based on asym-metric potential st-ochastic resonance. Measure. Control. **52**(5–6), 625–33 (2019). https://doi.org/10.1177/0020294019830435
13. W. Zhang, P. Shi, M. Li et al., Signal detection bas-ed on se-cond order underdamped tristable stocha-stic resonance an-d its application to weak fault di-agnosis. IEEE Access. **7**, 173753–173765 (2019). https://doi.org/10.1109/ACCESS.2019.2955605
14. Z. Li, X. Liu, T. He et al., A periodic potential underdamped stochastic resonance method and its application for gear fault diagnosis. IEEE Access. **7**, 141633–141647 (2019). https://doi.org/10.1109/ACCESS.2019.2943191
15. L. He, C. Tan, G. Zhang, Research on standard three-well stochastic resonance system and its application in early bearing fault diagnosis. Europ. Phys. J. Plus. **136**(7), 1–19 (2021). https://doi.org/10.1140/epjp/s13360-021-01741-0
16. Z. Yang, Z. Li, F. Zhou et al., Weak fault feature extraction method based on improved stochastic resonance. Sensors. **22**(17), 6644 (2022). https://doi.org/10.3390/s22176644
17. D. Huang, J. Yang, D. Zhou et al., Novel adaptive search m-ethod for bearing fault frequency using st-ochastic resonance quantified by amplitude-doma-in index. IEEE Trans. Instrument. Measure. **69**(1), 109–121 (2019). https://doi.org/10.1109/TIM.2019.2890933
18. H. Cui, Y. Guan, H. Chen et al., A novel advancing signal processing method based on coupled multi–stable stochastic resonance for fault detection. Appl. Sci. **11**(12), 5385 (2021). https://doi.org/10.3390/app11125385
19. P. Shi, W. Zhang, D. Han et al., Stochastic resona-nce in a high order time-delayed feedback tristabl-e dynamic system and its application. Chaos, Solitons & Fractals. **128**, 155–166 (2019). https://doi.org/10.1016/j.chaos.2019.07.048

20. S. Zhao, P. Shi, D. Han, A novel mechanical fault signal feature extraction method based on unsatur-ated piecewise tri-stable stochastic resonance. Measurement. **168**, 108374 (2021). https://doi.org/10.1016/j.measurement.2020.108374
21. J. Tang, B. Shi, Z. Li et al., Weak fault feature extraction method based on compound tri-stable stochastic resonance. Chin. J. Phys. **66**, 50–59 (2020). https://doi.org/10.1016/j.cjph.2020.05.009
22. L. He, X. Zhou, T. Zhang, Stochastic resonance characteristic analysis of new potential function under Levy noise and bearing fault detection. Chin. J. Phys. **56**(2), 538–560 (2018)
23. G. Zhang, Y. Zhang, T. Zhang et al., Stochastic re-sonance in an asymmetric bistable system driven by multiplicative and additive Gaussian noise and i-ts application in bearing fault detection. Chin. J. Phys. **56**(3), 1173–1186 (2018). https://doi.org/10.1016/j.cjph.2018.04.022
24. P. Shi, M. Li, W. Zhang et al., Weak signal enhancement for machinery fault diagnosis based on a novel adaptive multi-parameter unsaturated stochastic resonance. Appl. Acoust. **189**, 108609 (2022). https://doi.org/10.1016/j.apacoust.2021.108609
25. L. He, C. Jiang, Analysis of asymmetric piecewise linear stochastic resonance signal processing model based on genetic algorithm. Complexity. (2020). https://doi.org/10.1155/2020/8817814
26. Z. Li, X. Liu, X. Wang et al., A multi-parameter constrained potential underdamped stochastic resonance method and its application for weak fault diagnosis. J. Sound Vibrat. **459**, 114862 (2019). https://doi.org/10.1016/j.jsv.2019.114862
27. B. Wang, F. Gao, M.K. Gupta et al., Risk analysis of a flywheel battery gearbox based on optimized stochastic resonance model. J. Energy Storage. **52**, 104926 (2022). https://doi.org/10.1016/j.est.2022.104926
28. T. Gong, J. Yang, M.A.F. Sanjuán et al., Adaptive stochastic resonance for bolt looseness identification under strong noise background. J. Computat. Nonlinear Dyn. **17**(7), 071003 (2022). https://doi.org/10.1115/1.4053799
29. X. Zhang, J. Wang, Z. Liu et al., Weak feature enhancement in machinery fault diagnosis using empirical wavelet transform and an improved adaptive bistable stochastic resonance. ISA Trans. **84**, 283–295 (2019). https://doi.org/10.1016/j.isatra.2018.09.022
30. C.U. Mba, V. Makis, S. Marchesiello et al., Condition monitoring and state classification of gearboxes using stochastic resonance and hidden Markov models. Measurement. **126**, 76–95 (2018). https://doi.org/10.1016/j.measurement.2018.05.038
31. J. Kim, R.L. Harne, K.W. Wang, Online signal denoising using adaptive stochastic resonance in parallel array and its application to acoustic emission signals. J. Vibrat. Acoust. (2022). https://doi.org/10.1115/1.4052639
32. H. Cui, Y. Guan, W. Deng, Fault diagnosis using cascaded adaptive second-order tristable stochastic resonance and empirical mode decomposition. Appl. Sci. **11**(23), 11480 (2021). https://doi.org/10.3390/app112311480
33. H. Cui, Y. Guan, H. Chen et al., A novel advancing signal processing method based on coupled multistable stochastic resonance for fault detection. Appl. Sci. **11**(12), 5385 (2021). https://doi.org/10.3390/app11125385
34. J. Li, J. Zhang, M. Li et al., A novel adaptive stochastic resonance method based on coupled bistable systems and its application in rolling bearing fault diagnosis. Mechan. Syst. Signal Process. **114**, 128–145 (2019). https://doi.org/10.1016/j.ymssp.2018.05.004
35. T. Gong, J. Yang, S. Liu et al., Non-stationary feature extraction by the stochastic response of couple-d oscillators and its application in bearing fault dia-gnosis under variable speed condition. Nonlinear Dyn. **108**(4), 3839–3857 (2022). https://doi.org/10.1007/s11071-022-07373-y
36. L.F. He, Y.Y. Cui, T.Q. Zhang et al., Analysis of weak signal detection based on tri-stable system under Levy noise. Chin. Phys. B. **25**(6), 060501 (2016). https://doi.org/10.1088/1674-1056/25/6/060501
37. N.Q. Hu, Theory and methods for detection of weak signals with random resonance. National Defense Indust. Press. **1**, 300–303 (2012)

Publisher's Note Springer Nature remains neutral with regard to jurisdictional claims in published maps and institutional affiliations.

Springer Nature or its licensor (e.g. a society or other partner) holds exclusive rights to this article under a publishing agreement with the author(s) or other rightsholder(s); author self-archiving of the accepted manuscript version of this article is solely governed by the terms of such publishing agreement and applicable law.